Dynamic Additive Manufacturing onto Free-Moving Human Anatomy via Temporal Coarse/Fine Control

Anna French, John O'Neill, Ryan Madson, and Timothy M. Kowalewski

***Abstract*—The ability to deposit fluids with viable cells onto unfixtured free-moving substrate or non-planar unconstrained anatomy can enable a new class of medical procedures in fields such as reconstructive surgery, cosmetic treatments, and skin grafting. To this end, this work investigates a visual servo, temporal coarse/fine approach to 3D printing on the human hand using low-cost hardware kinematically optimized to match empirically recorded hand dynamics. Temporal coarse/fine shows a significant improvement in print area of a target point as compared to traditional techniques.**

I. INTRODUCTION

Surgery has traditionally focused on removal of tissue, effectively a subtractive manufacturing process. While reconstructive surgery aims to build up tissue this is usually done be removing existing tissue from alternate sites either from the same patient, like tissue grafts, or possibly from external sources like donor patients, animals, or synthetic organs. To date, surgeons lack the ability to additively manufacture biomaterials *in situ* in addition to traditional subtractive methods like resection or selective ablation. We herein propose a new approach of dynamic additive manufacturing for medical applications. This is where a robotically actuated end effector that combines a print head and tracking sensor synchronizes its motion with free moving anatomy like a hand, pulsing blood vessel, or beating heart and precisely deposits material.

Additive manufacturing is a rapidly growing technology which has shown promise in medical applications [1]. Application areas include organ implants, tissue engineering, and drug delivery [2]. Recently, Boland et al. used inkjet printers for printing cells via HP Deskjet printers [3]. In all of these cases precise positioning is necessary but often costly. As a result, additive manufacturing has historically been constrained to only deposit material onto rigidly fixtured nondeformable bodies. Although modern sensors provide fast sampling rates at a relatively low cost, actuation speeds to match such rapidly-sensed events come at a high price. In applications with a binary actuation task where the actuator only fires if correctly positioned, only the binary actuator requires a high bandwidth. In cases where increased time to complete the task is allowable, our proposed temporal coarse/fine control could be used to complete the printing task without expensive or complicated actuators. Temporal coarse/fine refers to motor driven positioning of the end effector roughly over the target point, with sensors more accurately checking when the end effector is coincident on the target and depositing material. This could also have applications in additive manufacturing in uncertain environments, where stopping or starting the stream of material could be much faster than the bulk motion of the print head. If the target is moving, temporal control can allow arbitrary accuracy, allowing for a long enough time scale to cross all target points with adequate accuracy.

Previous work by O'Neill et al. [4] shows the benefits of end-effector sensing for closely tracking a human hand. The system used a Leap Motion controller (Leap Motion, Inc. San Francisco, CA) to track a hand and a felt tip pen to draw on the hand for evaluation of accuracy and stability. However, the pseudo-metrics used to determine accuracy did not expand well beyond the single point at the center of the hand. The tracker and pen were mounted on the end effector of a large 3DOF robot that was kinematically optimized for setting up robotic surgery[5] and not for the motions of a human hand. Additionally, the pen used did not allow for quick disengagement of the tool, and as such the large latency in the system led to less accurate control than is desired, especially for quick accelerations, which can be beyond 10g[6]. The delicate interaction force required between the felt tip marker and the human subject could not be controlled by the robot, thus the system was not completely automated. Additional work in [7] demonstrated printing on an unfixtured hand using hydrogels using piezo microjetting. However, the size of the orifice depositing the material was 50-600μm, significantly larger than that of an inkjet at 20μm.

The hardware design investigated here has the Leap Motion sensor rigidly attached to the end effector, much like hardware that performs visual servoing. Visual servo control has been investigated by Hutchinson et al.[8]. This deals with control of the robot joints based on the information from a camera either on the robot or in a global system. Stable visual servoing of camera-in-hand robotic systems has been investigated by Kelly et al.[9]. This paper focused on an environment with static objects, and not dynamic targets, such as the human hand.

The accuracy and repeatability of tool tracking for the Leap Motion was independently analyzed by Weichert et.al[10]. These results show a static accuracy of 0.2 mm in 3D space, and that an accuracy of below 2.5 mm could be obtained for dynamic systems. However it should be noted that this test was done on a preliminary development version of the Leap Motion and only measured its accuracy in tracking a tool.

Further research investigates uncalibrated visual servoing[11]. This involves dynamically observing a

A. French, R. Madson, and T. Kowalewski are with the Department of Mechanical Engineering, University of Minnesota, Minneapolis, MN 55455 USA. J. O'Neill is with the Department of Medical Physics and Biomedical Engineering at University College London. Questions can be directed to afrench at umn dot edu.

978-1-5386-2512-5/18/$31.00

Figure 1: Solid model rendering of kinematically optimized two link robot design

Figure 2: Experimental Setup, CORVUS robot used to repeatably play back prerecorded hand motions

quasi-static target while actuating joints to build an observed Jacobian. Control is then achieved through that Jacobian. If the initial estimate of the Jacobian is sufficiently close to the true value, then convergence is guaranteed. However, a large initial error can lead to divergence [12]. This investigation assumes an estimate of the motor positions from the encoder to calculate the Jacobian, and re-evaluates the Jacobian each time a new encoder reading becomes available. This removes the issues with error accumulation.

Coarse/fine controllers have been investigated by Hollis et al.[13] and Kwon et al.[14] for high-bandwidth large-workspace applications. They utilize high-speed small-workspace actuators to provide redundant actuation at a high rate, which corrects for the slow dynamics of the base actuators and also successful at tracking shaking targets. However, both experiments used expensive, redundant actuators to achieve fast response times, and thus required twice as many actuators as degrees of freedom. The redundant actuators also required a complicated and integrated control scheme to coordinate the system and keep the fine actuators within their small workspace.

By placing the sensing at the end effector and actuating only when the end effector is coincident on a desired target point, specified target points on a moving object can be serviced with minimalistic control and hardware while accuracy of the printed image can be maintained. The utility of this method is demonstrated by using the approach to print binary images on a moving human hand, using a two-link planar robot arm for the coarse control of the inkjet position and the Leap Motion sensor for the fine control in deciding when the inkjet should fire.

II. METHODS

A. Hardware Design

Figure 2 shows the experimental setup. An inkjet was placed at the distal end of a two degree of freedom planar robot arm, allowing the robot to track a human hand in 2D. The planar arm was constructed of a laser-cut pattern of $6mm$ cast acrylic, and the link lengths were optimized to minimize length while still meeting the requirements of matching the kinematics of a human hand over a workspace of a $50mm$ square. The minimum singular value decomposition was chosen as the metric of manipulability; placing a bound on this value can ensure that the velocity requirement is satisfied in any direction. Based on the desired kinematics, the minimum effective radius was found to be $159mm$. Using a bisection search, the optimal link lengths were found to be $L1 = 228mm$ and $L2 = 228mm$. Dynamixel MX-64T servomotors (ROBOTIS Ltd. Seoul, South Korea) were used to actuate the arm, connected to an OpenCM 9.04 development controller board (ROBOTIS Ltd.), which was also used for communicating with the inkjet.

The Leap Motion sensor shown in Figure 3 was used to determine the position and orientation of the hand reference frame with respect to the Leap Motion frame. The Leap Motion sensor and the InkShield were mounted to the same rigid body so their relative position was constant.

In order to provide a repeatable human hand movement, a 45 second recording was made of the position of a hand held unsupported over the Leap Motion (an author served as the subject). Two recordings were made: the first with the subject attempting to remain as stationary as possible, the second holding the arm in a relaxed position, allowing the hand to wander more significantly. The first saw an average of velocity of $6mm/s$ and over a $16x7mm$ area, the second saw an average velocity of $40mm/s$ over a $120x70mm$ area. This motion was then played back on a 3-axis robot, CORVUS [4]. A mannequin hand was attached to the end effector and the trajectory was looped to provide continuous motion of the hand for the experiments, where the two-link robot had no knowledge of the trajectory being played back and relied only on the sensor data.

B. Software Design

The robot is fed a rasterized image of the desired print. For this application, all images were outlines only one pixel in width. Print order for the pixels contained in the image are chosen by selecting the leftmost pixel and commencing in a clockwise fashion along the string of pixels. The center of mass of the image is placed at the origin of the hand, and the desired positions of the pixels are commanded accordingly. The two-link robot is fed commands to place the printhead

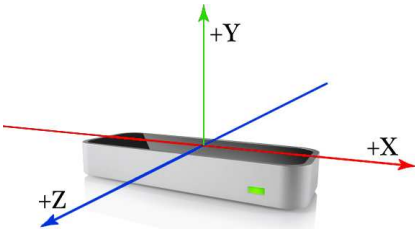

Figure 3: Leap Motion sensor, courtesy of Leap Motion

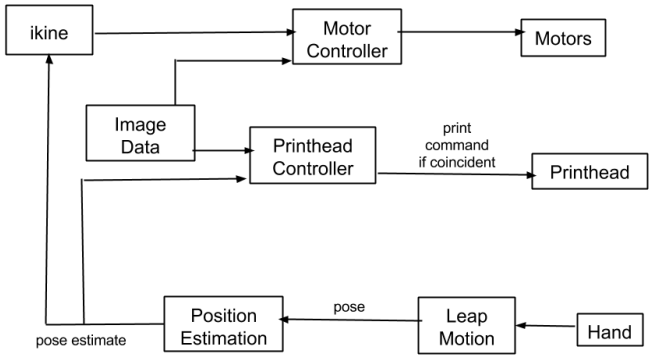

Figure 4: Control flow chart

coincident on each pixel, and attempts to deposit ink for a discrete period of time, moving on either once the printhead has fired or the timeout period is reached.

The decision to fire the printhead was made using one of two different methods: the "standard" method or temporal corase/fine. Under the "standard" method, the motors are commanded to a particular position and told to fire once that position has been obtained. Under the temporal/coarse fine method, in addition to maneuvering the motors to a particular desired print position, the hand position from the Leap Motion is also monitored throughout the maneuver. If a desired print position is detected by the Leap Motion (i.e. not just the current target pixel), ink is deposited.

Since inking pixels in a two-tone image need not be done in a particular order, the controller can choose to actuate whenever the printhead is coincident on a high pixel. Given this flexibility, it is not necessary to have an actuator capable of moving the printhead to particular positions on the hand quickly. Instead, the system can rely more on the comparatively faster sensing loop and the inherent motion of the hand, reducing the cost of the overall system by using slower actuators. Although simple inverse kinematics are used to lead the printhead mounted on the tool tip to points on the hand that require ink, the temporal coarse/fine approach dissociates inaccuracy in the encoders and sag in the arm from the accuracy of the printed point. This is the case since the inking decision is only made based on the position sensed by the Leap Motion, which is rigidly attached to the printhead. The control flow is shown in Figure 4.

C. Experimental Design

The performance of temporal coarse/fine control was compared to classical end effector sensing control scheme in four experiments. In all experiments, the target is considered to be the back side of a human hand, onto which material from an inkjet must be deposited. We use a standard inkjet with black ink in order to easily visualize the results. A nitrile surgical glove was used on top of the mannequin hand in order to allow multiple experimental runs as well as to provide an easy way to store the results from each experiment. The target was considered to be within $1mm$ of the ideal point, which is the range that the robot used to determine whether or not to apply ink.

To better quantify the tracking error for a hand, a preliminary tests was conducted recording the 3D palm position and velocity perceived by the Leap Motion of a stationary mannequin hand. The Leap Motion delivered a new estimate of the position of the hand's center of mass every $8.8ms$ on average. The mannequin hand and the Leap Motion controller were each held in a fixed position and the position of the hand was recorded for 2.5 hours under constant lighting conditions to observe what type of variability in position of the hand the Leap Motion perceives, both in the 2D plane that the robot operates in, and the vertical dimension as well.

Each of the following experiments was performed with and without temporal coarse/fine control, and results comparing coarse/fine to traditional are compared for precision.

1) Experiment 1: Playback of the human hand which was held approximately steady, with normal hand motion. The robot was programmed to apply the ink to a single point on the back of the hand. The test ran for $60s$ for each control scheme. Figure 5 shows the path traced by the steady hand playback.

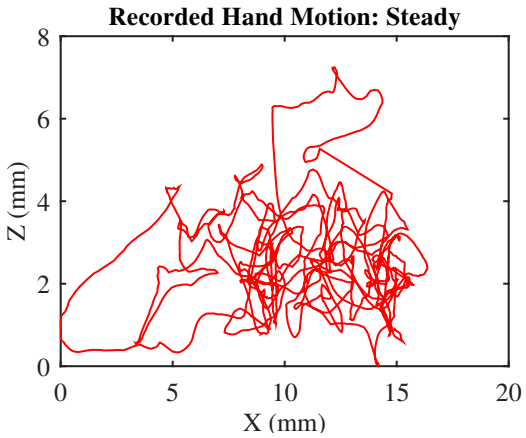

Figure 5: Steady hand path trace ($6mm/s$ average speed)

2) Experiment 2: Playback of the human hand performing free motions, moving up to approximately $50mm$ at the widest deviation in the path. The robot was programmed to apply the ink to a single point on the back of the hand, and the test ran for $60s$ for each control scheme. Figure 6 shows the path traced by this hand playback.

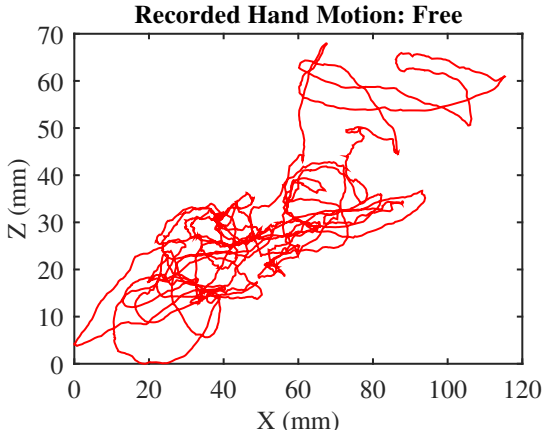

Figure 6: Free hand path trace ($40mm/s$ average speed)

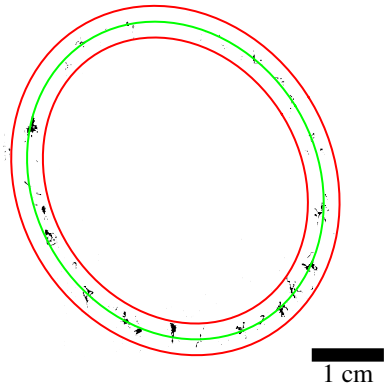

Figure 7: Example of ellipse fit

3) Experiment 3: Playback of the steady hand. The robot was programmed to apply the ink to a series of points around a circle of $25mm$ in diameter in $.17rad$ increments. The robot spent $10s$ targeting each point, resulting in a total test time of $6min$.

4) Experiment 4: Playback of the free motion, with the same circle pattern and timing commanded as with Experiment 3.

5) Digital Analysis: For all experiments the inked gloves were digitized using a fixed camera setup. The images were manually converted to binary by applying a threshold to the grayscale image, and errant shadows from creases and the grain of the gloves were removed. All experiments used the summation of the high pixels in the binary image to find the area of the printed spot. Experiments 1 and 2 used a mean to find a center, and a circle of $2.7mm$ was placed around the center point, and points within the circle were considered acceptable. Experiments 3 and 4 used a least squares fit to the conic equation of the ellipse to the data. This was because the data from all test runs followed the same elliptical skew. This best fit ellipse was then expanded inwards and outwards by $2.7mm$ to give a bounded region of acceptable points. This can be seen in Figure 7 with the best fit ellipse shown in green, and the bounding ellipses are shown in red.

III. RESULTS

The preliminary sensor accuracy test with no robot motion provided a standard deviation of $1.7mm$ in the 2D plane of interest. The standard deviation in vertical position, which is not tracked by the robot, was observed as $3.7mm$.

Figure 8 shows the result from Experiment 1, where the mannequin hand was programmed with steady hand motion, and the target was a single dot. The figure shows the dot for the standard control (left) with an area of $24.4mm^2$, and the dot for the temporal coarse/fine control (right) with an area of $8.5mm^2$.

Figure 9 shows the result from Experiment 2, where the mannequin hand was programmed with free hand motion, and the target was a single dot. The figure shows the dot for the standard control (left) with an area of $243.0mm^2$, and the dot for the temporal coarse/fine control (right) with an area of $49.3mm^2$.

Figure 10 shows the result from Experiment 3, where the mannequin hand was programmed with steady hand motion, and the target was a circle. Figure 11 shows the distribution of radii about the center of the best-fit ellipse for each mode, with green showing points within the tolerance range and red showing points outside the tolerance range.

Figure 12 shows the result from Experiment 4, where the mannequin hand was programmed with free hand motion, and the target was a circle. Figure 12 shows the distribution of radii about the center of the best-fit ellipse for each mode, with green showing points within the tolerance range and red showing points outside the tolerance range.

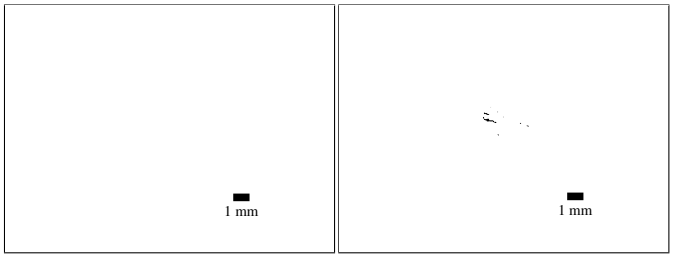

(a) Standard control (b) Temporal coarse/fine

Figure 8: Experiment 1 dot shape, steady motion results

Table I: Print area of commanded pixel $[mm^2]$

Experiment	Pattern	Hand Motion	Standard Control	Temporal Coarse Fine Control
Dot	1	Steady	10.2	0.6
	2	Free	80.0	0.5
Circle	3	Steady	336.3	30.6
	4	Free	248.0	4.9

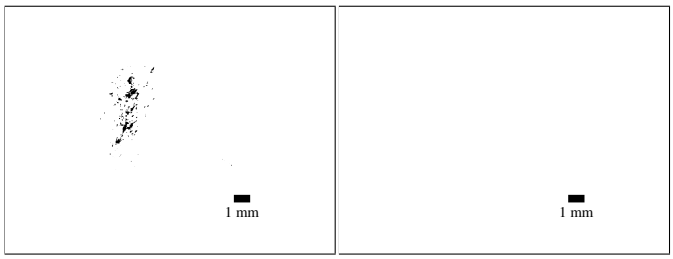

(a) Standard control (b) Temporal coarse/fine

Figure 9: Experiment 2 dot shape, free motion results

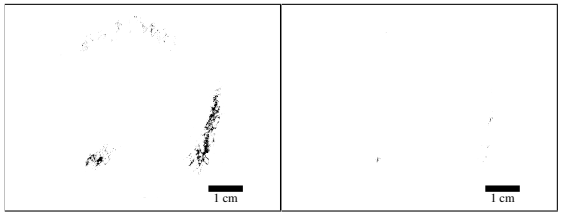

(a) Standard control (b) Temporal coarse/fine

Figure 10: Experiment 3 circle shape, steady motion results

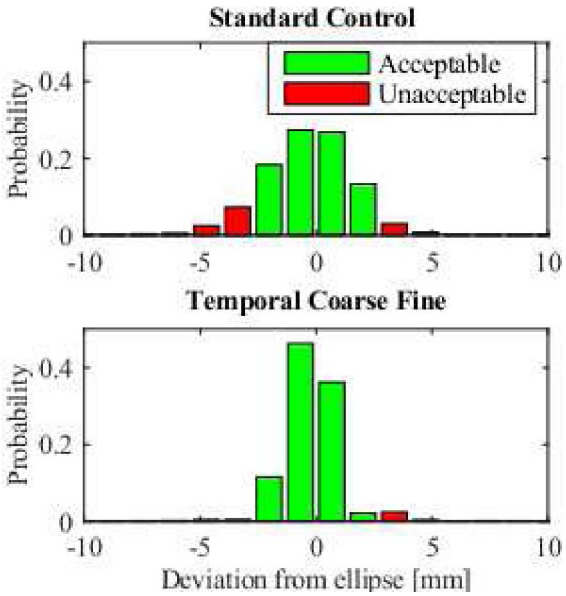

Figure 11: Exp 3: Steady motion

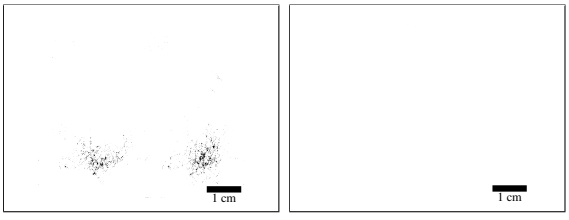

(a) Standard control (b) Temporal coarse/fine

Figure 12: Experiment 4 circle shape, free motion results

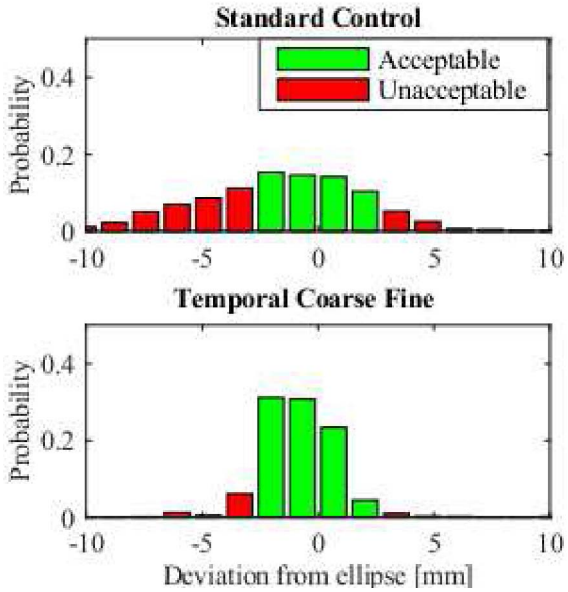

Figure 13: Exp 4: Free motion

Table II: Precision to target

Experiment	Pattern	Hand Motion	Standard Control	Temporal Coarse Fine Control
Dot	1	Steady	90.0%	90.3%
	2	Free	28.6%	81.6%
Circle	3	Steady	73.0%	93.6%
	4	Free	42.6%	81.5%

IV. DISCUSSION

The results show that a significant increase in the precision of the application of material from an inkjet is possible through the use of a temporal coarse/fine controller. However, the results scale with hand motion, as Experiment 1 only showed a virtually insignificant increase in precision of less than a percentage point while Experiment 2, with more hand motion, showed a 185% increase in precision. This is further exemplified by the results of Experiments 3 and 4, which showed a 12% increase in precision for the steady hand and 65% decrease for the free moving hand, as can be seen in Figure 14.

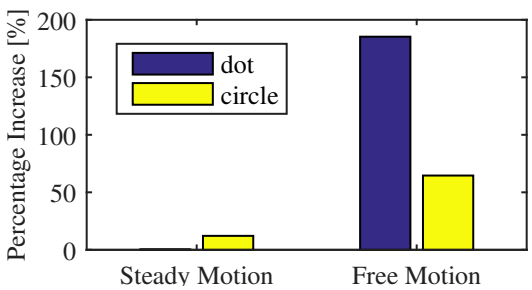

Figure 14: Precision improvement of temporal coarse/fine over standard control

However, the improved precision of the coarse/fine controller comes at the expense of an increased time to apply the same amount of material, as can be seen by the fact that more than $10\times$ more material was applied within the fixed time of the experiments.

The results also show that the controller and optimized planar robot abilities extend beyond one single point, and should work with any arbitrary shape or collection of pixels, provided that enough time is given to reach the points. For example, see Figure 15 for an application of an arbitrary shape onto a hand.

While the experiments in this paper used a mannequin hand for repeatability, the system works with real human hands as well, as can be seen in Figure 16 where experiment 3 was repeated on a human test subject. The inkjet used in this work is amenable to depositing human cells [3]. This indicates that, in principle, 3D bioprinting directly onto free moving anatomy is feasible.

Applications of this control scheme include areas where the accuracy/time trade-off can be made, such as in medical applications where the accurate delivery of medicine or cells could be much more important than speed.

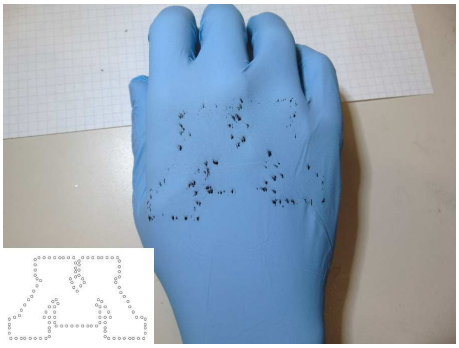

Figure 15: Printing a shape outline (see inert) under simulated steady hand motion

Figure 16: Printing of a $4cm$ diameter dotted circle on a human hand

V. CONCLUSION

This work demonstrates that temporal coarse/fine control can effectively trade off between precision and time in robotic printing applications. In principle, this renders 3D bio-printing directly onto free-moving human anatomy feasible.

Future work for this research will include extending to other anatomy beyond the human hand. This will require nonrigid registration and additional sensors beyond the Leap Motion sensor. In addition, the fast tracking ability of the Delta robot [15] could improve tracking speed for this application, using a design where the InkShield and Leap Motion are rigidly mounted on a common structure at the end effector of the Delta.

REFERENCES

[1] F. P. Melchels, M. A. Domingos, T. J. Klein, J. Malda, P. J. Bartolo, and D. W. Hutmacher, "Additive manufacturing of tissues and organs," *Progress in Polymer Science*, vol. 37, no. 8, pp. 1079–1104, 2012.

[2] N. Guo and M. C. Leu, "Additive manufacturing: technology, applications and research needs," *Frontiers of Mechanical Engineering*, vol. 8, no. 3, pp. 215–243, 2013.

[3] T. Boland, T. Xu, B. Damon, and X. Cui, "Application of inkjet printing to tissue engineering," *Biotechnology journal*, vol. 1, no. 9, pp. 910–917, 2006.

[4] J. J. O'Neill and T. M. Kowalewski, "Online free anatomy registration via non-contact skeletal tracking for collaborative human/robot interaction in surgical robotics," *ASME Journal of Medical Devices*, 2014.

[5] D. Friedman, T. Kowalewski, R. Jovanovic, J. Rosen, and B. Hannaford, "Freeing the serial mechanism designer from inverse kinematic solvability constraints," *Applied Bionics and Biomechanics*, vol. 7, no. 3, pp. 209–216, 2010.

[6] H. Nagasaki, "Asymmetric velocity and acceleration profiles of human arm movements," *Experimental Brain Research*, vol. 74, no. 2, pp. 319–326, 1989.

[7] J. J. O'Neill, R. A. Johnson, R. L. Dockter, and T. M. Kowalewski, "3d bioprinting directly onto moving human anatomy," in *Intelligent Robots and Systems (IROS 2017), 2017 IEEE/RSJ International Conference on*. IEEE, 2017.

[8] S. Hutchinson, G. D. Hager, and P. I. Corke, "A tutorial on visual servo control," *Robotics and Automation, IEEE Transactions on*, vol. 12, no. 5, pp. 651–670, 1996.

[9] R. Kelly, R. Carelli, O. Nasisi, B. Kuchen, and F. Reyes, "Stable visual servoing of camera-in-hand robotic systems," *Mechatronics, IEEE/ASME Transactions on*, vol. 5, no. 1, pp. 39–48, 2000.

[10] F. Weichert, D. Bachmann, B. Rudak, and D. Fisseler, "Analysis of the accuracy and robustness of the leap motion controller," *Sensors*, vol. 13, no. 5, pp. 6380–6393, 2013.

[11] J. A. Piepmeier, G. V. McMurray, and H. Lipkin, "Uncalibrated dynamic visual servoing," *Robotics and Automation, IEEE Transactions on*, vol. 20, no. 1, pp. 143–147, 2004.

[12] ——, "Tracking a moving target with model independent visual servoing: a predictive estimation approach," in *Robotics and Automation, 1998. Proceedings. 1998 IEEE International Conference on*, vol. 3. IEEE, 1998, pp. 2652–2657.

[13] R. L. Hollis, S. E. Salcudean, and A. P. Allan, "A six-degree-of-freedom magnetically levitated variable compliance fine-motion wrist: design, modeling, and control," *Robotics and Automation, IEEE Transactions on*, vol. 7, no. 3, pp. 320–332, 1991.

[14] S. Kwon, W. K. Chung, and Y. Youm, "On the coarse/fine dual-stage manipulators with robust perturbation compensator," in *Robotics and Automation, 2001. Proceedings 2001 ICRA. IEEE International Conference on*, vol. 1. IEEE, 2001, pp. 121–126.

[15] K. Hsu, M. Karkoub, M.-C. Tsai, and M. Her, "Modelling and index analysis of a delta-type mechanism," *Proceedings of the Institution of Mechanical Engineers, Part K: Journal of Multi-body Dynamics*, vol. 218, no. 3, pp. 121–132, 2004.